

## 全息中基于多算法融合的相位拼接方法研究

谢中思, 郭天太, 刘维\*, 孔明, 王道档, 郝玲

中国计量大学计量测试工程学院, 浙江 杭州 310018

**摘要** 为了解决数字全息中子孔径相位拼接的效率和精度问题, 提出了数字全息中基于多算法融合优化的相位拼接方法来实现相位的双方向拼接。首先, 在相位拼接中选用相位相关法确定重叠区域, 以限定特征点检测和提取范围, 从而提升特征点检测的速率和有效特征点检测的占比; 然后, 对重叠区域进行 Harris 角点检测和角点匹配, 并根据角点匹配点对来缩小块匹配算法的搜索范围; 最后, 采用全匹配搜索算法对最佳角点匹配点进行精确匹配, 并通过加权融合实现三维形貌的再现相位拼接。实验结果表明, 本文算法能够在保证较高的拼接精度的情况下, 极大地提高相位拼接的效率。

**关键词** 全息; 相位拼接; 相位相关法; Harris 角点检测算法; 块匹配

中图分类号 O438.1

文献标志码 A

doi: 10.3788/CJL202148.0709001

### 1 引言

数字全息技术是用 CCD 或 CMOS 等光电探测器件来代替传统光学全息的记录干板进行全息图的记录, 并将全息图传入计算机, 用数字仿真的方法再现全息图<sup>[1-3]</sup>。与此同时, CCD 或 CMOS 等光电传感器件的阵列尺寸和像素总数也限制了数字全息的成像视场及再现像的质量, 影响了数字全息技术应用范围的扩展。而目前数字全息获得大视场图像的方法主要有全息图拼接和相位拼接, 全息图拼接主要是获取物体不同区域的子全息图, 然后利用图像拼接技术合成一幅大范围的全息图, 再进行重建从而获得物体的大范围信息, 但是全息图清晰度较低, 且有很大的噪声影响, 所以全息图拼接停滞不前<sup>[4]</sup>。相位拼接技术<sup>[5-6]</sup>——将全息图进行重建和相位解包裹之后得到物体的正确相位图像进行拼接, 提供了一种在不大幅度增加数字全息实验光路系统难度的情况下, 明显增加检测视场大小和提高三维图像质量的方法。

图像配准是图像拼接的核心部分, 主要包括基于灰度的配准和基于特征的配准<sup>[7-9]</sup>。在传统图像拼接领域, 基于灰度配准的配准精度高, 但其对灰度

变化较为敏感, 尤其是非线性化的光照变化, 将降低算法的性能, 而且它的计算复杂度高, 对被测对象的旋转、形变以及遮挡比较敏感; 基于特征匹配可以改善上述方法的缺陷, 其用于匹配的特征点远少于原图的像素点, 大大减少了匹配过程的计算量, 而且特征点匹配对位置变化较为敏感, 对噪声的干扰、灰度的变化、图像的形变和遮挡等有较好的适应能力, 但其配准效率和特征搜索精度难以同时保证<sup>[10-15]</sup>。

对数字全息的相位拼接而言, 数字全息图解包裹得到的子孔径相位图像较小, 无旋转、无尺度变化, 且图像质量易受光路系统中噪声的影响<sup>[16-18]</sup>。在数字全息相位拼接领域中, 传统块匹配算法在相位图进行多次拼接之后, 块匹配的拼接效率将随着拼接相位图尺寸的增加而大幅度下降, 并且块匹配在相位图相似区域极易发生误配现象; 与此同时, 传统角点检测算法在整幅图像提取角点, 存在不必要的角点检测和提取, 会导致配准耗时过大, 且影响配准精度。

为了保证相位拼接的效率、精度以及拼接的成功率, 本文将相位相关法<sup>[19-21]</sup>、Harris 算法<sup>[22-23]</sup>和全匹配搜索(FS)算法<sup>[24]</sup>从图像拼接领域引入数字全息的相位拼接中, 提出了一种数字全息中基于多算法融合优化的相位拼接方法, 有效解决了灰度配

收稿日期: 2020-09-09; 修回日期: 2020-10-12; 录用日期: 2020-10-29

基金项目: 国家自然科学基金(51775528)

\*E-mail: liuw@cjlu.edu.cn

准算法存在的计算时间较长、适应性较差、相似部分容易发生误配的问题,同时保证了特征匹配算法的配准效率、特征搜索精度和拼接的成功率,提高了数字全息测量效率和测量精度,有效扩大了数字全息被测物体的测量面积。

## 2 基于多算法融合优化的相位拼接方法

针对传统 Harris 角点检测算法在整幅图像提取角点存在的问题,本文算法选用相位相关法确定各子孔径相位图的重叠区域,显著缩小了 Harris 角点检测的范围,提高了 Harris 角点检测的效率,同时避免了对无效角点的检测,进一步提升角点的配准精度。相位相关法算法简单、运行速度快、抗干扰

能力强,但在利用该算法进行重叠区域计算时,需保证各子孔径相位图的重叠区域不小于 50%,否则将会影响相位相关法的计算准确性<sup>[25]</sup>。

之后,使用 Harris 算法对相位图重叠区域进行角点检测。同时,针对 Harris 角点检测算法抗噪能力差、散斑噪声会导致出现伪角点的问题,本文算法再对 Harris 角点邻域的相位信息进行分析,剔除平坦区域、噪声点、边缘引起的伪角点<sup>[26]</sup>。

伪角点剔除后,本文算法通过归一化互相关函数(NCC)<sup>[27]</sup>进行特征点配准。以每个特征点为中心,取一个  $N \times N$  大小的相关窗口,设参考图像第  $i$  个特征点和输入图像中第  $j$  个特征点对应的窗口像素的相位值分别是  $I_1(x, y)$  和  $I_2(x, y)$ ,通过归一化互相关函数进行特征点匹配,计算公式为

$$C_{NC}(i, j) = \frac{\sum_{x=1}^N \sum_{y=1}^N [I_1(x, y) - \bar{I}_1] [I_2(x, y) - \bar{I}_2]}{\sqrt{\sum_{x=1}^N \sum_{y=1}^N [I_1(x, y) - \bar{I}_1]^2 \sum_{x=1}^N \sum_{y=1}^N [I_2(x, y) - \bar{I}_2]^2}}, \quad (1)$$

式中:  $I_1$  和  $I_2$  为两幅图窗口内相位的平均值。

$C_{NC}$  的值域为  $[-1, 1]$ ,  $C_{NC} = -1$  表示两个相关窗口完全不相似,  $C_{NC} = 1$  表示两个窗口完全相同,当  $C_{NC}$  值大于阈值时认为特征点匹配。但是,基于 NCC 匹配的方法受光照、尺度变换、噪声影响时,其匹配准确率会降低。因此,本文算法根据引导互匹配法<sup>[28]</sup>和投票过滤法剔除误配的点。随后,根据剔除误配点对后的各 Harris 角点匹配点对的  $C_{NC}$  值,选择  $C_{NC}$  最大值对应的匹配点对作为最佳匹配点对,并利用全匹配搜索算法对相位图进行精确匹配。

全匹配搜索算法是对每一个像素点(搜索范围内)进行匹配运算,最后找到各子孔径相位图的平移量,是搜索精度最高的算法。全匹配搜索算法以最佳匹配点对所对应的特征点为中心,在参考图像中选取一个  $N \times N$  大小的块区域作为参考模板,在输入图像中选取一个  $2N \times 2N$  大小的块区域作为搜索区域,先从搜索区域的中心点出发,按照由近及远顺时针的方向,在搜索区域范围内在所有像素点的位置处利用 SAD 匹配准则<sup>[29-31]</sup>来计算每个像素点对应的  $D_{SA}(i, j)$  值,计算公式为

$$D_{SA}(i, j) = \sum_{s=1}^N \sum_{t=1}^N |f_k(s, t) - f_{k-1}(s+i, t+j)|, \quad (2)$$

式中:  $f_k(s, t)$  和  $f_{k-1}(s, t)$  为参考模板和匹配区域的像素,  $(s, t)$  为像素坐标,匹配块的大小为  $N \times N$ ,  $(i, j)$  为匹配块相对参考块的偏移量。最小  $D_{SA}$  值对应的偏移量即对应最佳匹配块,则各子孔径相位图的偏移量可由参考模板和最佳匹配块的初始点坐标差得到。同时,全匹配搜索算法简单、可靠,找到的匹配块必为全局最优点。匹配后根据计算出的偏移量对非重叠区域进行平移,同时采用加权平均法对重叠区域进行处理,从而得到被测物体的拼接相位分布图。

如图 1 所示,本文算法不仅使用相位相关法提高了 Harris 的检测效率,还通过全匹配搜索算法进行精确匹配的方法来消除 Harris 匹配点对存在的误差,同时由于 Harris 算法是基于检测窗口内各方向的灰度变化情况来检测角点,避免了全匹配搜索算法存在的相似区域发生误配的情况,而且基于小窗口的块匹配,在保证拼接精度的情况下解决了块匹配存在的匹配效率较低的问题。

## 3 实 验

### 3.1 实验平台

为检验本文算法,采用反射式离轴数字全息实验系统进行验证,实验光路图如图 2(a) 所示,系统实物图如图 2(b) 所示。其中, He-Ne 激光器型号为

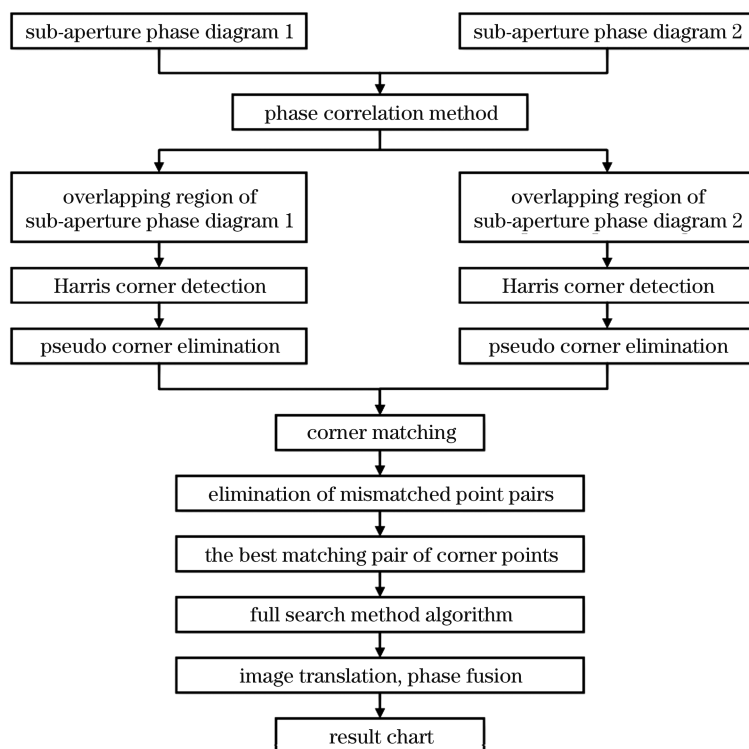
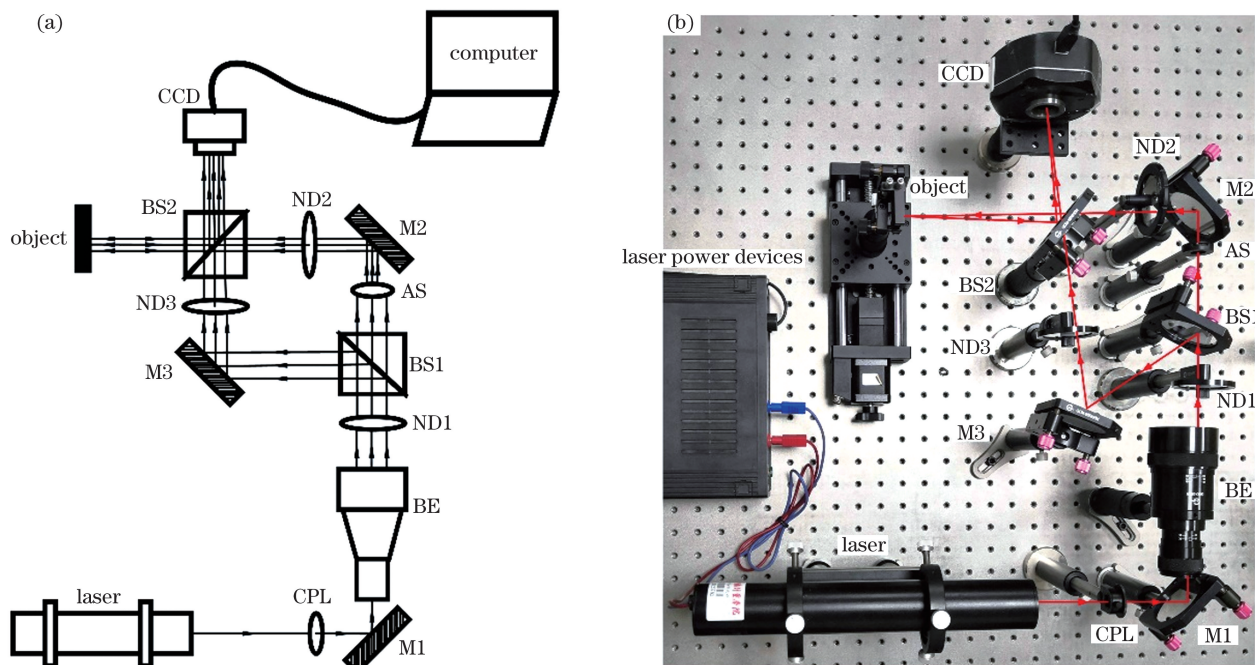


图 1 算法流程图

Fig. 1 Algorithm flow chart



CPL: circular-polarizing lens; M: mirror; BE: collimating beam expanding system; ND: ND filter; BS: beam splitter; AS: aperture stop

图 2 反射式离轴数字全息实验系统。(a)实验光路图;(b)数字全息装置

Fig. 2 Reflective off-axis digital holography experimental system. (a) Experimental light path diagram; (b) digital holography setup

DH-HN250, 波长为 632.8 nm, CCD 的像元尺寸为  $2.775 \mu\text{m} \times 2.775 \mu\text{m}$ , 以刻有“a”字样 (3 mm × 3 mm) 的玻璃样板作为被测样本。

如图 2 所示, 输入的 He-Ne 激光经过偏振后, 被反射镜反射进入扩束准直镜, 经准直扩束系统 (BE) 和分光镜 (BS1) 分成两束, 其中, 一束激光通过

衰减滤光片(ND3)之后作为参考光,另一束激光通过衰减滤光片(ND2)之后经物体反射形成物光。物光和参考光经过分光镜(BS2)之后,在 CCD 表面产生干涉条纹形成全息图,并被 CCD 记录,最后图像传输到计算机上做进一步的处理。分光器的作用主要是控制物光和参考光的夹角。光阑主要作为记录物体光斑尺寸大小的控制器,同时分离分光镜前后表面反射产生的光束,防止多光束干涉。衰减片的作用主要是控制物光和参考光的光强比,在光学全息中,一般情况下,为了产生预定的偏置曝光量,参考光强应大于物光光强。特别是在拍摄三维物体时,如果物光过强,则由于散斑效应会在全息相位图上出现散射现象。ND 为连续可调衰减片,由于宽光束会造成光强分布不均,所以在实验中需要适当调节衰减片,使得参考光和物光的光强比均在

1:1~2:1 的范围内。

受光斑大小限制,系统无法采集到完整的被测区域。因此,通过图 2 所示反射式离轴数字全息实验系统记录四幅子孔径全息图,并通过计算机模拟光波衍射,再根据菲涅耳积分公式<sup>[32]</sup>解析再现像的包裹相位,随后进行最小二乘相位解包裹<sup>[33]</sup>获得相应的子孔径再现相位分布图,最后利用本文提出的算法进行拼接。记录时,保持 CCD 固定不动,在垂直于光轴的面内将被测物体进行二维平移,采集被测物体四个部分的全息图,相邻部分应保留至少 50% 的重叠区域。图 3(a)~(d)为采集到的各子孔径的全息图,经衍射计算重构物光场,对重构的物光场进行相位提取,然后通过多项式拟合的方式实现全息面倾斜像差的补偿<sup>[34-36]</sup>,得到各子孔径再现相位分布图,如图 3(e)~(h)所示。

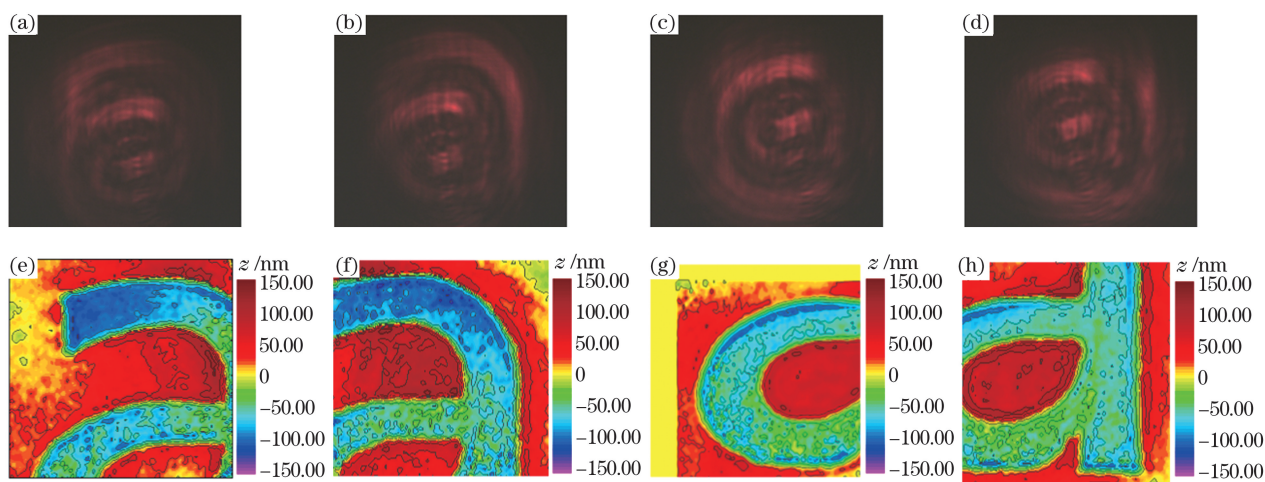


图 3 各子孔径的全息图和再现相位分布图。(a)~(d)各子孔径全息图;(e)~(h)各子孔径再现相位分布图

Fig. 3 Holograms and reproduced phase distributions of each sub-aperture. (a)~(d) Holograms of each sub-aperture; (e)~(h) reproduced phase distributions of each sub-aperture

### 3.2 基于多算法融合优化的相位拼接实验

本实验采用层次式的拼接方式,对四幅子孔径相位图先进行  $x$  方向的横向拼接,分别获得“a”字样的上半部分和下半部分,再进行  $y$  方向的纵向拼接,获取拼接的整体相位分布图。根据数字全息干

涉原理,表面尺寸与相位值存在一一对应的映射关系,由此可计算得到被测物件的表面尺寸值。

以图 4 所示纵向拼接为例,图 4(a)和图 4(b)分别为横向拼接后获得的“a”字样的上半部分和下半部分的相位分布图。

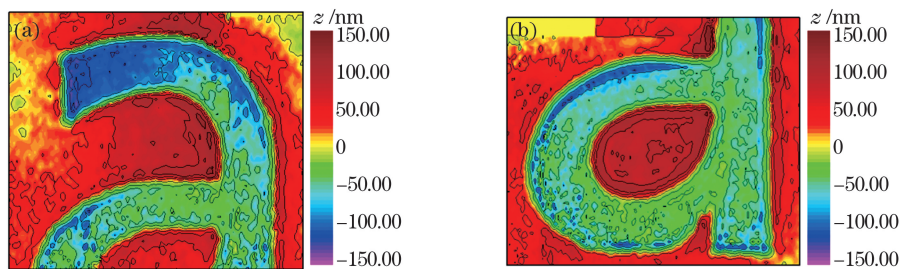


图 4 纵向拼接子孔径相位分布图。(a)上半部分相位分布图;(b)下半部分相位分布图

Fig. 4 Phase distributions of sub-aperture of longitudinal splicing. (a) Upper half phase distribution; (b) lower half phase distribution

先使用相位相关法获得子孔径相位图重叠区域如图 5(a)和图 5(b)所示,再使用 Harris 算法对各子孔径相位图重叠区域进行角点检测,所得角点如图 5(c)和图 5(d)所示,然后根据角点邻域相位信息剔除由平坦区域、噪声点、边缘引起的伪角点,结果如图 5(e)和图 5(f)所示。观察图 5(a)和图 5(b)可

知,相位相关法大幅度缩小了角点检测的区域,可有效提高特征点检测的效率及进一步提高后续的配准精度。对比图 5(c)、(e)及图 5(d)、(f)可知,基于角点邻域相位信息可有效滤除平坦区域、散斑噪声、边缘引起的伪角点。

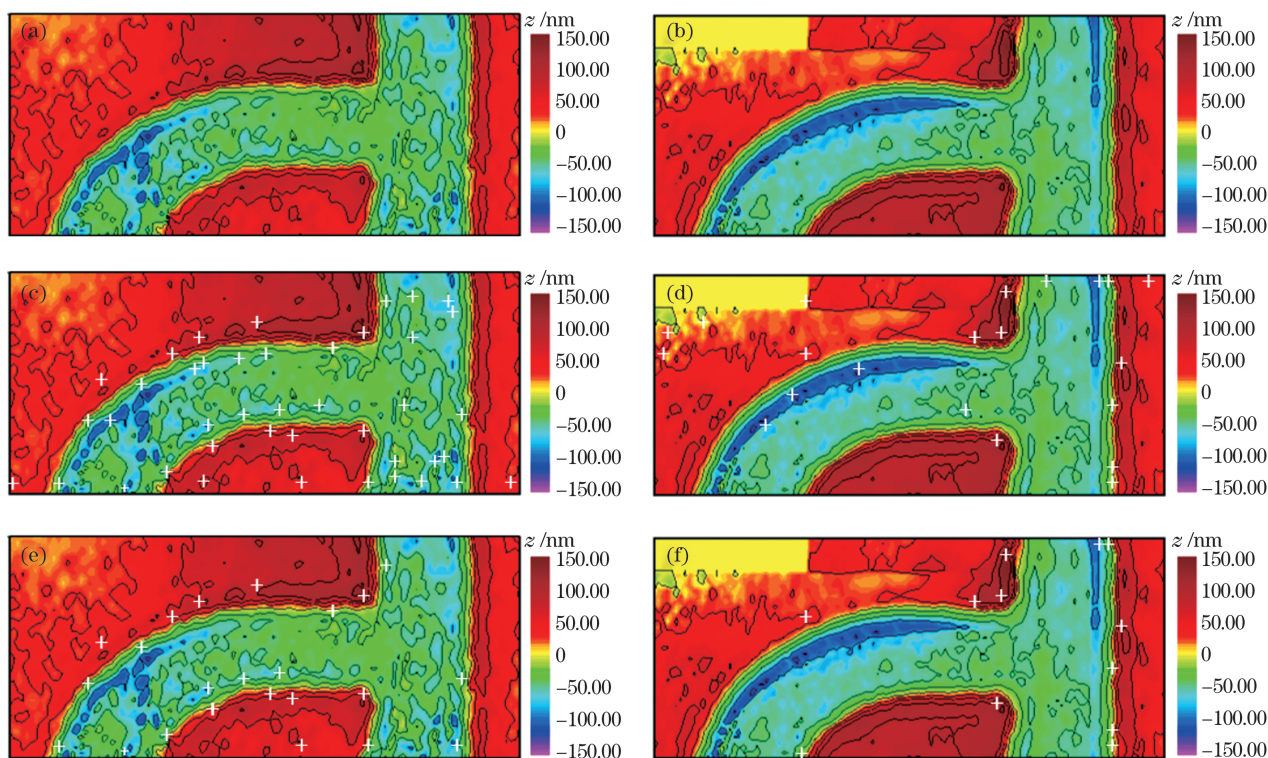


图 5 纵向拼接重叠区域角点检测及滤波。(a)(b)子孔径相位图重叠区域;(c)(d)重叠区域 Harris 角点检测;(e)(f)Harris 角点滤波

Fig. 5 Corner detection and filtering in overlapping area of longitudinal splicing. (a)(b) Overlapping region of sub-aperture phase diagram; (c)(d) Harris corner detection in overlapping region; (e)(f) Harris corner filtering

使用归一化互相关函数对两幅子孔径相位图像检测到的角点进行配准,配准结果如图 6(a)所示,随后根据引导互匹配法和投票过滤法剔除误配点对,如图 6(b)所示,再根据剔除误配点对后的各 Harris 角点匹配点对的 NCC 值获得 Harris 最佳匹配点对,如图 6(c)所示,最后根据最佳匹配点对使用全匹配搜索算法获得精准配准,计算出两子相位图的相对偏移量以及相应的重叠区域。

匹配后根据计算出的偏移量对非重叠区域进行平移,同时采用加权平均法对重叠区域进行相位融合,得到玻璃样板上“a”字样的再现强度图和相位分布图。同时,分别使用 Harris 算法、尺度不变特征变换(SIFT)算法、Susan 算法和全匹配搜索算法对玻璃样板上“a”字样的各个子孔径相位图

进行相位拼接,得到玻璃样板上“a”字样的再现强度图和相位分布图。图 7 为各相位拼接算法结果比较。

通过对比图 7(a)~(e)中各算法拼接结果的再现强度图可观察到,“a”字样已经拼接完成。结合比较各个算法的再现强度图、相位分布图可见,基于 Harris 算法的相位拼接存在明显的误差,基于 Susan 算法的相位拼接结果出现极大的错位,相比之下,SIFT 算法、全匹配搜索算法和本文算法的拼接结果较好。此外,取图 7(f)~(j)中相位分布图  $x=70$  pixel 的截面曲线图(如相位分布图竖线所示)与日本东京精密株式会社的精密粗糙度测量仪(型号 S1910DX3)测得的截面曲线图进行比较,如图 8 所示。

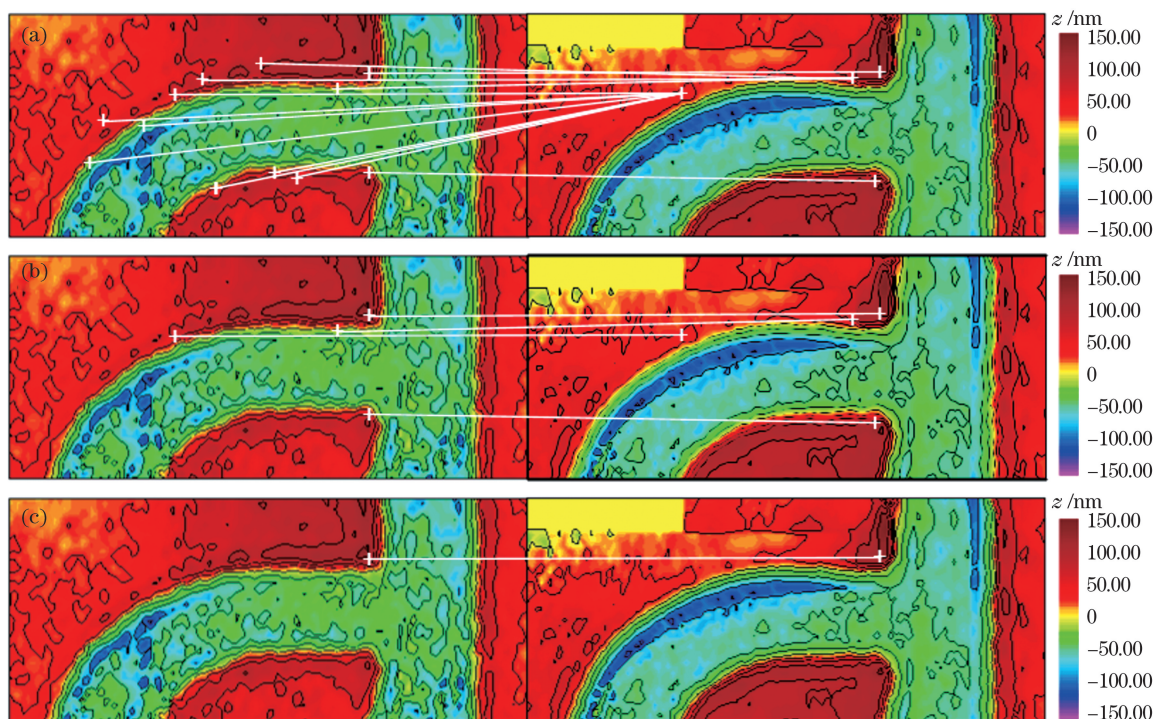


图 6 纵向拼接特征点配准。(a)NCC 特征点配准图;(b)误配点对剔除效果图;(c)最佳匹配点对

Fig. 6 Registration of feature points of longitudinal splicing. (a) Feature point registration map of NCC algorithm; (b) result chart of mismatch point pair elimination; (c) best match point pair

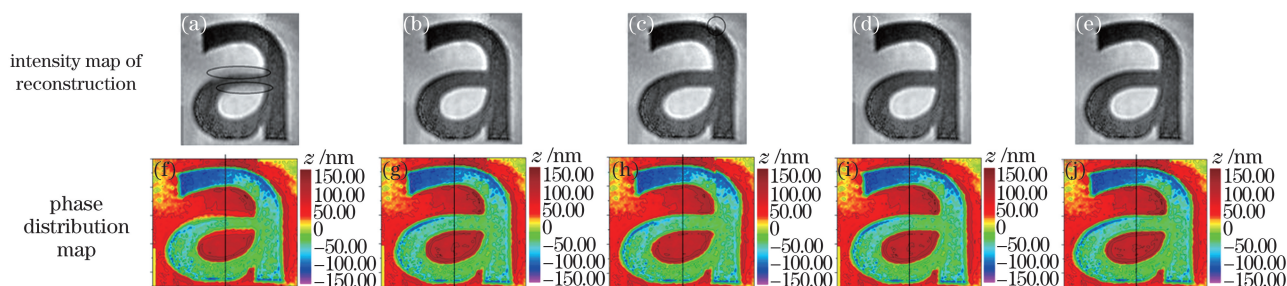


图 7 各相位拼接算法结果比较。(a)(f) Harris;(b)(g) SIFT;(c)(h) Susan;(d)(i) FS;(e)(j) 本文算法

Fig. 7 Comparison of the results of each phase stitching algorithms. (a)(f) Harris; (b)(g) SIFT; (c)(h) Susan; (d)(i) FS; (e)(j) proposed algorithm

如图 8 截面曲线对比图所示,各算法拼接结果的相位分布图与东京精密粗糙度测量仪测得的截面曲线图的“a”字样高度参数均在 $\pm 150$  nm 之间;由于全息图相位解包裹存在误差,直接影响各算法的拼接相位分布图,分析可知后面两个高度参数为“-”的区域存在较多误差点,而中间两个高度参数为“+”的区域相位误差点较少。为了便于观察,取如图 8 所示截面曲线的局部放大图进行分析,基于 Harris 算法的相位拼接误差较大,基于 Susan 算法的相位拼接结果出现极大的错位;相比之下,SIFT 算法、全匹配搜索算法和本文算法的拼接结果较好。

此外,为了进一步比较图 7 中各个算法的拼接精度,取各算法拼接相位分布图与 SEVEN OCEAN

Accura III 影像测量仪测得的影像图进行轮廓对比分析。先对各个算法以及影像图进行 Prewitt 算子边缘检测,得到图 10 所示轮廓图。随后对各个轮廓图进行 Hu 距计算,得到 7 个 Hu 不变矩,并进行对数处理后作为特征匹配向量<sup>[37]</sup>。最后,采用欧氏距离与余弦相似度对各个轮廓图和影像图的 Hu 距特征匹配向量进行相似度计算。欧氏距离与个体各维度的特征数值直接相关,距离越小,两图像之间越相似;而余弦相似度体现的是方向上的差异,余弦相似度越大,两图像之间越相似。比较结果如表 1 所示,本文算法得到的相位分布图与影像测量仪测得的影像图轮廓最为相似,Harris 算法所得相位分布图与影像图相似性最低。

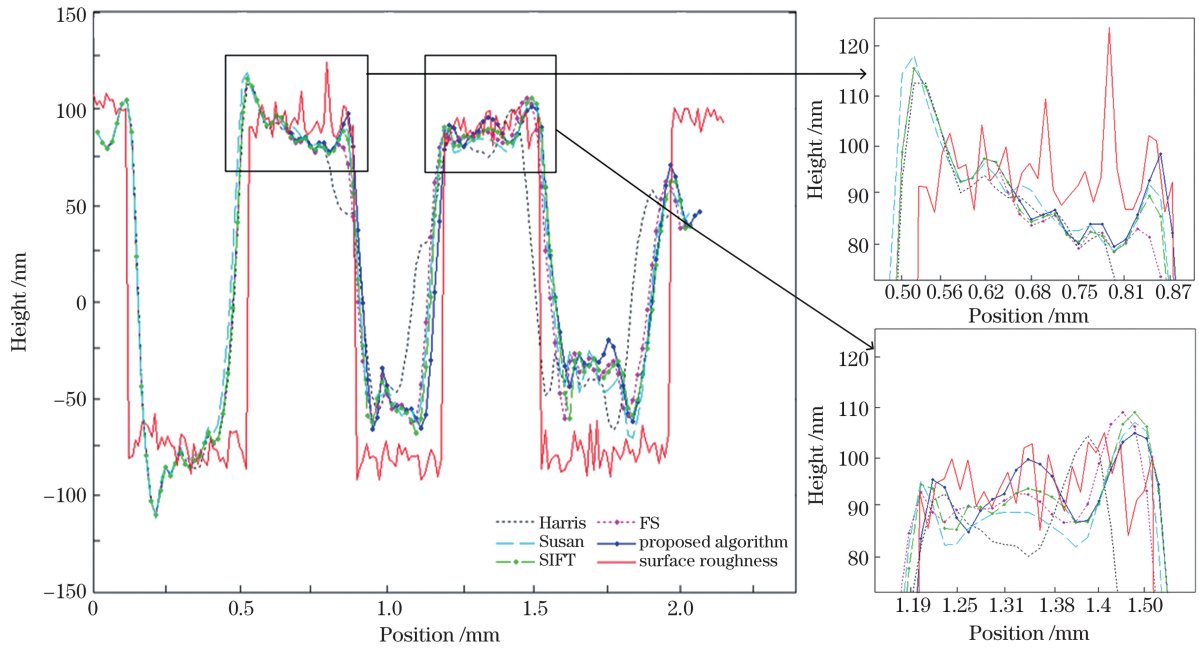


图 8 截面曲线图

Fig. 8 Section curve map



图 9 影像测量仪测得的影像图

Fig. 9 Image measured by image measuring instrument

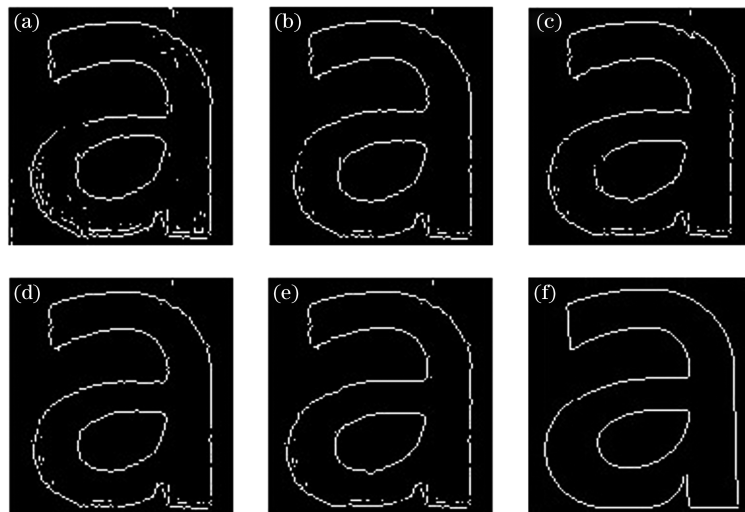


图 10 Prewitt 算子边缘检测轮廓图。(a) Harris; (b) SIFT; (c) Susan; (d) FS; (e) 本文算法; (f) 影像图

Fig. 10 Prewitt operator edge detection image contour. (a) Harris; (b) SIFT; (c) Susan; (d) FS; (e) proposed algorithm; (f) image map

表 1 各算法与影像图的轮廓相似性比较

Table 1 Comparison of structural similarity between each algorithm and image map

Algorithm	Harris	SIFT	Susan	FS	Proposed algorithm
Cosine similarity	0.245	0.838	0.725	0.740	0.914
Euclidean distance	9.318	5.250	5.850	4.806	3.615

### 3.3 实验结果分析

匹配成功率和匹配时间可体现算法的有效性、适用性和效率。本文算法从以上两个方面与经典 Harris

算法、SIFT 算法、Susan 算法、全匹配搜索算法进行了对比,通过对 50 组不同的实验数据使用上述各个算法进行层次式拼接,所得拼接结果如表 2 所示。

表 2 各相位拼接算法的数据对比

Table 2 Data comparison of each phase splicing algorithm

Algorithm	Harris	SIFT	Susan	FS	Proposed algorithm
Matching success rate /%	40.00	38.00	48.00	28.00	80.00
Matching time /s	1.636	59.916	15.321	2.830	1.689

在本实验所采用的实验拼接结果中,对测量仪测得的影像图和各拼接算法得到的拼接相位图进行轮廓比较,如图 7(a)、(f)所示 Harris 算法和图 7(c)、(h)所示 Susan 算法对应的再现强度图和相位分布图,其轮廓偏差超过 5 pixel,从而导致相位拼接出现明显的误差或错位,即认定为匹配失败;如图 7(b)、(g)所示 SIFT 算法,图 7(d)、(i)所示全匹配搜索算法和图 7(e)、(j)所示本文算法对应的再现强度图和相位分布图,即为匹配成功。分析表 2 可知:基于 SIFT 算法、Susan 算法相位拼接的效率较低;Harris 算法具有较高抗鲁棒性,匹配效率高,但其极易受噪声影响而出现伪角点和角点簇,匹配存在一定误差;SIFT 算法的匹配精度较高,但其匹配效率低,在数字全息领域的全息相位图普遍不大的情况下,相位图中测得的 SIFT 角点数目较少,从而影

响配准精度,且层次式拼接引入新的误差也会进一步降低 SIFT 算法匹配成功率,导致 SIFT 算法在数字全息领域的应用得不偿失;Susan 算法由于需要手动调节阈值,所以无法保证层次式拼接的匹配成功率;全匹配搜索算法由于存在相似区域的误配问题,且匹配块的选择充满不确定性,所以其匹配成功率最低;本文算法在匹配成功率、匹配时间、抗鲁棒性上都具有良好的表现,在提高了配准效率的同时保证了配准精度。

本实验采用层次式方法进行拼接,即先对横向相邻的子孔径相位图(85 pixel×85 pixel)进行横向拼接,再对横向拼接的结果图(115 pixel×85 pixel)进行纵向拼接,最终获取整体拼接相位分布图(115 pixel×125 pixel),各算法进行层次式拼接的横向拼接匹配时间和纵向拼接匹配时间如表 3 所示。

表 3 各相位拼接算法进行层次式拼接的匹配时间

Table 3 Matching time of each phase stitching algorithm for hierarchical splicing

unit: s

Algorithm	Harris	SIFT	Susan	FS	Proposed algorithm
Horizontal splicing	0.509	18.031	3.920	0.687	0.539
Longitudinal splicing	0.618	23.854	7.481	1.456	0.623

由于纵向拼接的子孔径相位图的像素数量明显多于横向拼接所对应的子孔径相位图,分析表 3 可知:SIFT 算法、Susan 算法和全匹配搜索算法的匹配时间随着子孔径相位图像素数量的增加而急剧增加,而本文算法和 Harris 算法的匹配时间变化较小。

## 4 结 论

相位拼接是数字全息中扩大视场的有效手段。

Harris 角点检测算法对各子孔径进行的相位匹配拼接技术实现简单,但由于误差累积,拼接的结果有一定的误差;全匹配搜索算法具有简单易行、搜索精度高的优点,但其计算量较大,且相似区域容易发生误配;本文提出的数字全息中基于多算法融合优化的相位拼接方法结合了 Harris 算法和全匹配搜索算法各自的优点,在提高配准效率的同时保证了配准精度,又充分发挥了 Harris 算法的高抗鲁棒性特点,在高分辨率的拼接测量中具有较为广泛的应用



前景。

除解决上述关键问题以外,由于本文算法利用 Harris 算法进行角点检测,故本文算法并不要求物体具备强边缘,但是要求各子孔径相位图重叠区域有 Harris 特征角点的存在,否则本文算法将不再适用。

### 参 考 文 献

- [1] Corda R. Digital holography data compression[C]//2018 26th Telecommunications Forum (TELFOR), November 20-21, 2018, Belgrade, Serbia. New York: IEEE Press, 2018: 1-4.
- [2] Oh K J, Choo H G, Kim J. Analysis on digital holographic data representation and compression[C]//2016 Asia-Pacific Signal and Information Processing Association Annual Summit and Conference (APSIPA), December 13-16, 2016, Jeju, South Korea. New York: IEEE Press, 2016: 1-4.
- [3] Ren R Y, Jia Z H, Yang J, et al. Quasi-noise-free and detail-preserved digital holographic reconstruction [J]. IEEE Access, 2019, 7: 52155-52167.
- [4] Shui Y X. Research on 3D object contour fusion technology based on digital holography [D]. Chongqing: Chongqing University of Technology, 2019.  
税云秀. 基于数字全息三维物体轮廓融合技术研究[D]. 重庆: 重庆理工大学, 2019.
- [5] Kong M, Hao L, Liu W, et al. Phase splicing algorithm based on optimized Harris corner in digital holography [J]. Infrared and Laser Engineering, 2019, 48(11): 1126002.  
孔明, 郝玲, 刘维, 等. 数字全息中基于优化 Harris 角点的相位拼接算法[J]. 红外与激光工程, 2019, 48(11): 1126002.
- [6] Sun J S, Zhang Y Z, Chen Q, et al. Fourier ptychographic microscopy: theory, advances, and applications[J]. Acta Optica Sinica, 2016, 36(10): 1011005.  
孙佳嵩, 张玉珍, 陈钱, 等. 傅里叶叠层显微成像技术: 理论、发展和应用[J]. 光学学报, 2016, 36(10): 1011005.
- [7] Liu Z Y, Guo Y N, Feng Z, et al. Improved rectangle template matching based feature point matching algorithm[C]//2019 Chinese Control And Decision Conference (CCDC), June 3-5, 2019, Nanchang, China. New York: IEEE Press, 2019: 2275-2280.
- [8] Yao S Y, Wang X M, Zuo S. Fast feature point matching algorithm based on SURF [J]. Laser & Infrared, 2014, 44(3): 347-350.  
尧思远, 王晓明, 左帅. 基于 SURF 的特征点快速匹配算法[J]. 激光与红外, 2014, 44(3): 347-350.
- [9] Wang Z B, Yang Z K. Review on image-stitching techniques[J]. Multimedia Systems, 2020, 26(4): 413-430.
- [10] Osten W, Faridian A, Gao P, et al. Recent advances in digital holography[J]. Applied Optics, 2014, 53(27): G44-G63.
- [11] Xu C. Research of image recognition method based on block matching and applications [D]. Beijing: North China University of Technology, 2015.  
徐晨. 基于块匹配的图像识别方法研究及应用[D]. 北京: 北方工业大学, 2015.
- [12] Chen L, Han J, Zhang Y, et al. Real-time panoramic image mosaic via Harris corner detection on FPGA [C] // International Conference on Image and Graphics. Springer, Cham, 2015: 111-124.
- [13] Liu J L, Wang H Q, Wang K, et al. Spectral image registration method based on SURF maximum submatrix [J]. Laser & Optoelectronics Progress, 2019, 56(6): 063002.  
刘加林, 王慧琴, 王可, 等. 基于快速稳健特征最大子矩阵的光谱图像配准方法[J]. 激光与光电子学进展, 2019, 56(6): 063002.
- [14] Maik V, Chae E, Lee E, et al. Robust sub-pixel image registration based on combination of local phase correlation and feature analysis[C]//The 18th IEEE International Symposium on Consumer Electronics (ISCE 2014), June 22-25, 2014, JeJu Island, South Korea. New York: IEEE Press, 2014: 1-2.
- [15] Liu P F, Gao R X. Image stitching method based on phase correlation and improved SURF [J]. Software Guide, 2019, 18(11): 157-160, 164.  
刘鹏飞, 高如新. 基于相位相关法与改进 SURF 算法的图像拼接方法[J]. 软件导刊, 2019, 18(11): 157-160, 164.
- [16] Verpillat F, Joud F, Atlan M, et al. Digital holography at shot noise level[J]. Journal of Display Technology, 2010, 6(10): 455-464.
- [17] Li Q, Liu W, Wang D D, et al. Four-direction least-square phase unwrapping algorithm based on shearing interferometry and second derivative of quality weight [J]. Journal of Optoelectronics·Laser, 2018, 29(6): 618-626.  
李芹, 刘维, 王道档, 等. 基于二阶质量权的四向剪切相位解包裹算法[J]. 光电子·激光, 2018, 29(6): 618-626.
- [18] Montessor S, Picart P. Quantitative appraisal for noise reduction in digital holographic phase imaging [J]. Optics Express, 2016, 24(13): 14322-14343.

- [19] Wang R Y, Gao Z S, Zhu D, et al. Subaperture stitching interferometry based on the combination of the phase correlation and iterative gradient methods [J]. *Applied Optics*, 2020, 59(13): 4176-4182.
- [20] Zhang J, Wang C S, Liao W L. An image mosaics algorithm based on improved phase correlation [C] // 2009 International Conference on Environmental Science and Information Application Technology, July 4-5, 2009, Wuhan, China. New York: IEEE Press, 2009: 383-386.
- [21] Sun B Q, Jing D H. Application and optimization of phase correlation algorithm in real-time video mosaic [J]. *Science Technology and Engineering*, 2012, 12(26): 6618-6621.  
孙步强, 静大海. 相位相关法实现视频实时拼接的应用与优化 [J]. *科学技术与工程*, 2012, 12(26): 6618-6621.
- [22] Hong Y X, Jie Z Q, Zhao D D, et al. UAV image automatic mosaic method based on matching of feature points [C] // 2013 Chinese Automation Congress, November 7-8, 2013, Changsha, China. New York: IEEE Press, 2013: 33-36.
- [23] Babu V M M, Santha T. Efficient brightness adaptive deep-sea image stitching using biorthogonal multi-wavelet transform and Harris algorithm [C] // 2017 International Conference on Intelligent Computing and Control (I2C2), June 23-24, 2017, Coimbatore, India. New York: IEEE Press, 2017: 1-5.
- [24] Choudhury H A, Saikia M. Block matching algorithms for motion estimation: a performance-based study [M]. New Delhi: Springer, 2015: 149-160.
- [25] Zhou M L, Bai Z W, Yan X J. Design of the image mosaic system based on phase correlation method [J]. *Foreign Electronic Measurement Technology*, 2015, 34(5): 31-33.  
周美丽, 白宗文, 延小进. 基于相位相关法的图像拼接系统设计 [J]. *国外电子测量技术*, 2015, 34(5): 31-33.
- [26] Zhang L T, Huang X L, Lu L L, et al. Fast Harris corner detection based on gray difference and template [J]. *Chinese Journal of Scientific Instrument*, 2018, 39(2): 218-224.  
张立亭, 黄晓浪, 鹿琳琳, 等. 基于灰度差分与模板的 Harris 角点检测快速算法 [J]. *仪器仪表学报*, 2018, 39(2): 218-224.
- [27] Li H, Qin J H, Xiang X Y, et al. A Harris corner matching optimization algorithm combing adaptive threshold and forstner [J]. *Telecommunication Engineering*, 2018, 58(9): 1079-1085.  
李浩, 秦姣华, 向旭宇, 等. 结合自适应阈值与 Forstner 的 Harris 角点匹配优化算法 [J]. *电讯技术*, 2018, 58(9): 1079-1085.
- [28] Zhang S T, Li C, Li L Q. An improved method for eliminating false matches [C] // 2017 2nd International Conference on Image, Vision and Computing (ICIVC), June 2-4, 2017, Chengdu, China. New York: IEEE Press, 2017: 133-137.
- [29] Chen G, Niu Q Z. On classical BMA in motion estimation of image sequence [J]. *Computer Applications and Software*, 2012, 29(5): 147-151.  
陈宫, 牛秦洲. 图像序列运动估计中经典块匹配算法研究 [J]. *计算机应用与软件*, 2012, 29(5): 147-151.
- [30] Feng Y P, Li S, Dai M. An image matching algorithm based on sub-block coding [C] // 2009 Second International Workshop on Computer Science and Engineering, October 28-30, 2009, Qingdao, China. New York: IEEE Press, 2009: 599-603.
- [31] Cuevas E, Zaldívar D, Pérez-Cisneros M, et al. Block-matching algorithm based on differential evolution for motion estimation [J]. *Engineering Applications of Artificial Intelligence*, 2013, 26(1): 488-498.
- [32] Huang W L, Bai X, Liang H K, et al. Experimental investigation and resolution optimization of digital holographic optics [J]. *Physics Experimentation*, 2019, 39(4): 44-48.  
黄威龙, 白欣, 梁海坤, 等. 数字全息光学实验探究及再现清晰度优化 [J]. *物理实验*, 2019, 39(4): 44-48.
- [33] Qian X F, Zhang Y A, Li X Y, et al. Phase unwrapping algorithm based on mask and least-squares iteration [J]. *Acta Optica Sinica*, 2010, 30(2): 440-444.  
钱晓凡, 张永安, 李新宇, 等. 基于掩膜和最小二乘迭代的相位解包裹方法 [J]. *光学学报*, 2010, 30(2): 440-444.
- [34] Zhang X, Pan F, Yi X S, et al. Method of digital holography WFOV imaging based on phase stitching [J]. *Modern Electronics Technique*, 2013, 36(21): 96-99.  
张鑫, 潘锋, 伊小素, 等. 基于相位拼接的数字全息大视场成像方法研究 [J]. *现代电子技术*, 2013, 36(21): 96-99.
- [35] Feng F, Tian A L, Liu B C, et al. Full-field three-dimensional test for scratch defects using digital holographic scanning imaging system [J]. *Chinese Journal of Lasers*, 2020, 47(4): 0409003.  
冯方, 田爱玲, 刘丙才, 等. 基于数字全息扫描成像的划痕缺陷全场三维测试 [J]. *中国激光*, 2020, 47(4): 0409003.

- [36] Li M Y, Cao T F, Yuan X D, et al. Effect of reference surface error on subaperture stitching for flat optics[J]. Chinese Journal of Lasers, 2019, 46(12): 1204006.  
李萌阳, 曹庭分, 袁晓东, 等. 参考面误差对平面子孔径拼接的影响[J]. 中国激光, 2019, 46(12): 1204006.
- [37] Zhang J K. Design and implementation of a novel template matching algorithm invariant to rotation[D]. Harbin: Harbin Institute of Technology, 2013.  
张俊凯. 一种快速的旋转模板匹配算法的设计与实现[D]. 哈尔滨: 哈尔滨工业大学, 2013.

## Phase Splicing Method Based on Multi-Algorithm Fusion in Holography

Xie Zhongsi, Guo Tiantai, Liu Wei\*, Kong Ming, Wang Daodang, Hao Ling

College of Metrology and Measurement Engineering, China Jiliang University, Hangzhou, Zhejiang 310018, China

### Abstract

**Objective** In digital holography, CCD or CMOS photodetectors are used to record holograms instead of the traditional recording plate in optical holography. The holograms are reproduced through digital simulation. However, array size and the total number of pixels of CCD or CMOS photodetectors restrict the imaging field of view and quality of reconstructed images, limiting the widespread application of digital holography. The main methods to obtain a large field of view images include hologram splicing and phase splicing. The hologram-splicing method is affected by the clarity and noise of the hologram. However, phase stitching provides a method to increase the size of the detection field and improve the quality of three-dimensional (3D) images without increasing the difficulty of the experimental optical system for digital holography. In the field of digital holographic phase stitching, the conventional block-matching algorithm has the disadvantage that the splicing efficiency of block matching is significantly reduced with the increase in the size of the subaperture phase map after the phase image is stitched many times. Block matching is prone to mismatching in similar regions of the phase map. The conventional corner-detection algorithm extracts corners from the entire image with unnecessary corner detection and extraction, leading to excessive registration time consumption and affecting registration accuracy. To solve the problem of efficiency and accuracy of phase stitching of subaperture phase diagram in digital holography, a phase-stitching method based on multi-algorithm fusion optimization is proposed to realize two-way phase stitching in digital holography.

**Methods** In phase stitching, the phase correlation method is used to determine the overlapping area to limit the detection and extraction range of feature points, thus improving the feature point detection speed and the proportion of effective feature point detection. Harris corner detection is conducted for the overlapping area, and the pseudocorners caused by flat area, noise point, and edges are eliminated according to the phase information of the corner neighborhood. Then, the normalized cross-correlation function is applied for corner matching. Guided complementary matching and voting filtering methods are used to simultaneously eliminate mismatched corner-matching point pairs, and the corresponding best matching point pair is obtained. The search range of the small block matching algorithm is reduced according to the best corner-matching point pair. Finally, the full matching search algorithm is used to accurately match the best corner-matching point pair, and weighted fusion is adopted to realize the reconstruction and phase splicing of 3D topography.

The sub-aperture holograms of four parts of the letter “a” of glass sample plate are collected using the reflection off-axis digital holography experiment system; at least 50% overlapping area should be reserved in the adjacent holograms. Next, the diffraction of a light wave is simulated using a computer. The reconstructed image phase is analyzed using the Fresnel integral formula. The reconstructed image phase distribution is obtained using the least square phase unwrapping. Finally, Harris algorithm, scale-invariant feature transform (SIFT) algorithm, Susan algorithm, full search method, and the proposed algorithm are used to splice the phase map of each subaperture of the letter “a” of the glass template to obtain the intensity map and phase distribution map of the letter “a” of the glass template. The splicing experiment is conducted hierarchically, i.e., the transverse adjacent subaperture phase map (85 pixel × 85 pixel) is horizontally spliced, and then the resultant image (115 pixel × 85 pixel) is longitudinally spliced. Finally, the overall splicing phase distribution map (115 pixel × 125 pixel) is obtained.

**Results and Discussions** The experimental results showed that there are obvious errors in the phase stitching

based on the Harris algorithm; moreover, the phase splicing results based on Susan algorithm are greatly misplaced. However, the results of SIFT algorithm, full search method, and proposed algorithm are better (Fig. 7). To compare the splicing accuracy of each algorithm in Fig. 7, the phase distribution map of each algorithm is selected for contour comparison and analysis with the image measured using the image measuring instrument. The matching accuracy of the proposed algorithm is the highest (Table 1). The experimental matching results showed that the efficiency of phase stitching based on SIFT algorithm and Susan algorithm is low; Harris algorithm has high antirobustness and high matching efficiency, but it is easily affected by noise, resulting in false corners and corner clusters, and there are certain errors in matching. SIFT algorithm has high matching accuracy; however, its matching efficiency is low, and the hierarchical splicing introduces new errors. This further reduces the matching success rate of SIFT algorithm. Susan algorithm cannot guarantee the matching success rate for hierarchical splicing because of the need to manually adjust the threshold. The full search method algorithm has the lowest matching success rate due to the mismatch problem of similar regions, and the block matching selection is full of uncertainty. The proposed algorithm has the matching success rate, matching time, and robustness. It can improve the matching efficiency and ensure matching accuracy (Table 2). In addition, the algorithm reduces the influence of the size of the subaperture phase map on its matching efficiency (Table 3).

**Conclusions** Phase stitching is an effective method to enlarge the field of view in digital holography. The phase-matching stitching technique of the Harris corner detection algorithm for each subaperture is simple. However, the splicing result has a certain error due to error accumulation. The full search method has the advantages of simple operation and high search accuracy, but it has a large calculation quantity and is prone to mismatching in similar regions. In this study, the phase splicing method based on multi-algorithm fusion optimization in digital holography is proposed by combining the Harris algorithm and full search method points, which can improve the matching efficiency and accuracy. Moreover, it provides full play to the high robustness of the Harris algorithm and does not require objects to have strong edges. It has a wide application prospect in high-resolution mosaic measurement.

**Key words** holography; phase splicing; phase correlation method; Harris corner detection algorithm; block matching

**OCIS codes** 090.1995; 350.5030